

1 Metamorphism during temperature gradient with undersaturated advective
2 airflow in a snow sample

3
4 Pirmin Philipp Ebner^{1,2}, Martin Schneebeli^{2,*}, and Aldo Steinfeld¹

5 ¹ *Department of Mechanical and Process Engineering, ETH Zurich, 8092 Zurich, Switzerland*

6 ² *WSL Institute for Snow and Avalanche Research SLF, 7260 Davos-Dorf, Switzerland*

7
8
9 **Abstract**

10 Snow at or close to the surface commonly undergoes temperature gradient metamor-
11 phism under advective flow, which alters its microstructure and physical properties.
12 Time-lapse X-ray micro-tomography is applied to investigate the structural dynamics of
13 temperature gradient snow metamorphism exposed to an advective airflow in controlled
14 laboratory conditions. Cold saturated air at the inlet was blown into the snow samples and
15 warmed up while flowing across the sample. The temperature gradient in the sample was
16 around 50 K m^{-1} at maximum airflow velocity. The sublimation of ice for saturated air
17 flowing across the snow sample was experimentally determined via changes of the porous
18 ice structure in the middle-height of the snow sample. Sublimation has a marked effect
19 on the structural change of the ice matrix but diffusion of water vapor in the direction of
20 the temperature gradient counteracted the mass transport of advection. Therefore, the total
21 net ice change was negligible leading to a constant porosity profile. However, the strong
22 recrystallization of water molecules in snow may impact its isotopic or chemical content.

23 *Keywords:* snow, temperature gradient, metamorphism, advection, sublimation, tomography

24
25 **1. Introduction**

26 Snow has a complex porous microstructure and consists of a continuous ice structure
27 made of grains connected by bonds and inter-connecting pores (Löwe et al., 2011). It has
28 a high permeability (Calonne et al, 2012) and under appropriate conditions airflow
29 through the snow structure can occur (Sturm and Johnson, 1991) due to variation of sur-

* Corresponding author. Email: schneebeli@slf.ch.

30 face pressure (Colbeck, 1989; Albert and Hardy, 1995), simultaneous warming and cool-
31 ing, and induced temperature gradients (Sturm and Johnson, 1991). Both diffusive and
32 advective airflows affect heat and mass transport in the snowpack and influence chemical
33 concentrations (Gjessing, 1977; Waddington et al., 1996). Various airflow conditions in
34 a snow sample occur, namely: isothermal airflow, temperature gradient along the flow
35 direction, and temperature gradient opposite to the airflow (Fig. 1). Under isothermal
36 condition, the continuous sublimation and deposition of ice due to higher vapor pressure
37 over convex surfaces and lower vapor pressure over concave surfaces, respectively (Kel-
38 vin-effect) (Neumann et al., 2008; Ebner et al., 2014). However, applying a fully isother-
39 mal saturated airflow across a snow sample has been shown to have no influence on the
40 coarsening rate that is typical for isothermal snow metamorphism independently of the
41 transport regime in the pores (Ebner et al., 2015a). When applying a temperature gradient,
42 the effect of sublimation and deposition in the snow results from interaction between
43 snow temperature and the local relative humidity in the pores. If vapor is advected from
44 a warmer zone into a colder zone, the air becomes supersaturated, and some water vapor
45 deposits onto the surrounding ice grains. This leads to a change in the microstructure
46 creating whisker-like crystals (Ebner et al., 2015b). Whisker-like crystals are very small
47 ($\sim 10\text{-}30\ \mu\text{m}$) elongated monocrystals. A deposition rate of water vapor on the ice matrix
48 dependence on the flow rate was observed, reaching asymptotically a maximum rate of
49 $1.05 \cdot 10^{-4}\ \text{kg m}^{-3}\ \text{s}^{-1}$ (Ebner et al., 2015b). Contrarily, if the temperature gradient acts in
50 the opposite direction of the airflow, the airflow through the snow brings cold and rela-
51 tively dry air into a warmer area, causing that the pore space air becomes undersaturated,
52 and surrounding ice sublimates. Here, we investigate specifically this last effect.

53 Sublimation of snow is a fundamental process that affects its crystal structure (Sturm
54 and Benson, 1997), and thus is important for ice core interpretation (Stichler et al., 2001;
55 Ekaykin et al., 2009), as well as calculation of surface energy balance (Box and Steffen,
56 2001) and mass balance (Déry and Yau, 2002). Albert (2002) suggest that condensation
57 of water vapor will have a noticeable effect on the microstructure of snow using airflow
58 velocities, vapor transport and sublimation rates calculated using a two-dimensional fi-
59 nite-element model, which is also confirmed by a 3D phase-field model of Kaempfer and
60 Plapp (2009).. Neumann et al. (2009) determined that there is no energy barrier to be
61 overcome during sublimation, and suggest that snow sublimation is limited by vapor dif-
62 fusion into pore space, rather than by sublimation at crystal surface.

63 In the present work, we studied the surface dynamic of snow metamorphism under an
64 induced temperature gradient and saturated airflow in a controlled laboratory experi-
65 ments. Cold saturated air at around $-14\text{ }^{\circ}\text{C}$ was blown into the snow samples and warmed
66 up to around $-12.5\text{ }^{\circ}\text{C}$ while flowing across the sample. Sublimation of ice was analyzed
67 by in-situ time-lapse experiment with microcomputer tomography (micro-CT) (Pinzer
68 and Schneebeli, 2009; Chen and Baker, 2010; Pinzer et al., 2012; Wang and Baker, 2014;
69 Ebner et al., 2014) to obtain the discrete-scale geometry of snow. By using discrete-scale
70 geometry, all structures are resolved with a finite resolution corresponding to the voxel
71 size.

72 **2. Time-Lapse tomography experiments**

73 Temperature gradient experiments with fully saturated airflow across snow samples
74 (Ebner et al., 2014) were performed in a cooled micro-CT (Scanco Medical μ -CT80) at a
75 cold laboratory temperature of $T_{\text{lab}} = -15^{\circ}\text{C}$. Cold saturated air was blown into the snow
76 samples and warmed up while flowing across the sample. Aluminum foam including a
77 heating wire was used to generate the warm side of the snow, opposite to the entering
78 airflow. We analyzed the following flow rates: a volume flow of 0 (no advection), 0.3,
79 1.0, and 3.0 liter/min. Higher flow rates were experimentally not possible as shear stresses
80 by airflow destroyed the snow structure (Ebner et al., 2015a). Nature identical snow pro-
81 duced in a cold laboratory (Schleef et al., 2014) was used for the snow sample preparation
82 (water temperature: $30\text{ }^{\circ}\text{C}$; air temperature: $-20\text{ }^{\circ}\text{C}$). The snow was sieved with a mesh
83 size of 1.4 mm into a box, and was sintered for 27 days at -5°C to increase the strength.
84 The sample holder (diameter: 53 mm; height: 30 mm) was filled by cutting out a cylinder
85 from the sintered snow and pushing into the sample holder without mechanical disturb-
86 ance of the core. The snow samples were measured with a voxel size of $18\text{ }\mu\text{m}$ over 108
87 h with time-lapse micro-CT measurements taken every 3 h, producing a sequence of 37
88 images. The size of the cubic voxel size was $18\text{ }\mu\text{m}^3$. The innermost 36.9 mm of the total
89 53 mm diameter were scanned, and subsamples with a dimension of $7.2\text{ mm} \times 7.2\text{ mm} \times$
90 7.2 mm were extracted for further processing. The imaged volume was in the center of
91 the sample (Fig. 1 c)). A linear encoder with a resolution of less than 1 voxel was used to
92 verify that the scans were taken at the same position. The reconstructed micro-CT images
93 were filtered by using a $3 \times 3 \times 3$ median filter followed by a Gaussian filter ($\sigma = 1.4$,
94 support = 3). The Otsu method (Otsu, 1979) was used to automatically perform cluster-
95 ing-based image thresholding to segment the grey-level images into ice and void phase.

96 Morphological properties of the two-phase system were determined based on the exact
97 geometry obtained by the micro-CT. The segmented data were used to calculate a trian-
98 gulated ice matrix surface and tetrahedrons inscribed into the ice structure. Morphological
99 parameters such as porosity (ε) and specific surface area (SSA) were then calculated. An
100 opening-based morphological operation was applied to extract the mean pore size of each
101 micro-CT scan (d_{mean}) (Haussener et al., 2012). Morphological parameters such as poros-
102 ity, specific surface area and the initial mean pore size were extracted from the micro-CT
103 images to study the ice-air interface dynamic. As additional physical and structural pa-
104 rameter, the effective thermal conductivity k_{cond} was estimated by direct pore-level simu-
105 lations (DPLS) to determine the influence of changing microstructure. DPLS determined
106 the effective thermal conductivity by solving the corresponding mass and momentum
107 conservation equations (Kaempfer et al., 2005; Petrasch et al., 2008; Calonne et al., 2011;
108 Löwe et al., 2013).

109

110 **3. Results**

111 Time-lapse tomographic scans were performed with temperature gradients between
112 43-53 K m^{-1} (Table 1). Small fluctuations of the measured inlet and outlet temperature
113 were due to temperature regulation both inside the cold chamber and inside the micro-CT
114 (Ebner et al., 2014). A shift of $\Delta t < 10$ min between inlet and outlet temperature indicated
115 that a fast equilibrium between the temperature of the snow and the airflow was reached
116 (Albert and Hardy, 1995; Ebner et al., 2015b). The morphological evolution was similar
117 between all four experiments and only a slight rounding and coarsening was visually ob-
118 served, shown in Fig. 2. The change of structural change “ota 3” at 30 h is due to an error
119 in the scan. The initial ice grains did not change with time and the locations of sublimation
120 and deposition for “ota3” and “ota4” is shown in Fig. 3. Sublimation of 7.7 % and 7.6 %
121 of the ice matrix and deposition of 6.0 % and 9.6 % on the ice matrix were observed. The
122 data were extracted by superposition of vertical cross-sections at 0 and 108 hours with an
123 uncertainty of 6%. The mass sublimated preferentially at locations of the ice grain with
124 low radii and was relocated leading to a smoothing of the ice grain and to an increase in
125 the size of pores (Fig. 4 a)). The pore size (uncertainty ~6 %) increased by 3.4 %, 3.6 %, 3.6 %,
126 5.4 % and 6.5 % for ‘ota1’, ‘ota2’, ‘ota3’, and ‘ota4’, respectively.

127 Loss of ice of the snow due to sublimation could not be detected by the micro-CT
128 scans due to limited accuracy and no flow rate dependence was observed during any of

129 the four experiments. The temporal evolution of the porosity, shown in Fig. 4 b), did not
130 change with time and the influence of sublimation of water vapor was not observed. Only
131 ‘ota2’ showed a slight drop in the temporal evolution of the porosity until 18 h into the
132 experiment but kept constant afterwards. This slight drop ($\approx 0.5\%$) was probably caused
133 by settling of the snow. A coarsening was observed for each experiment but the influence
134 of changing airflow was not visible, confirmed by the temporal SSA evolution, shown in
135 Fig. 4 c).

136 The repositioning of water molecules led to a smoothing of the ice grains, but did not
137 affect the thermal conductivity of snow. This quantity (standard deviation $\sim 0.025\text{ W m}^{-1}$
138 (Calonne et al., 2011)) slightly increased after applying airflow to the temperature gradi-
139 ent, shown in Fig. 4 d), but no flow rate dependence was observed. Every third scan was
140 used to extract the thermal conductivity and a change of -2.6% , 3.6% , 2.2% , and 2.7%
141 for ‘ota1’, ‘ota2’, ‘ota3’, and ‘ota4’ was detected.

142

143 **5. Discussion**

144 The rate of deposition onto the ice surface depends on the flow rate where warm sat-
145 urated air cooled down while flowing through the sample, as shown in previous experi-
146 ments (Ebner et al., 2015b). Its deposition rate asymptotically reached a maximum of 1.05
147 $\cdot 10^{-4}\text{ kg m}^{-3}\text{ s}^{-1}$. In this study, changing the temperature gradient leads to a warming up
148 of a cold saturated flow, and resulted in a sublimation rate too small for the analyzed
149 period of the experiment to measure a flow rate dependence by the micro-CT and an
150 influence on the temporal density gradient. A smoothing of ice grains and an increase of
151 the pore space was measured but the airflow velocity did not affect the relocation process
152 of water molecules.

153 A structural change of the ice grains and repositions of water molecules was observed
154 but the total net flux of the snow was not affected. The superposition of vertical cross-
155 section in Fig. 3 shows a big effect on reposition of water molecules on the ice structure.
156 However, the temporal porosity (Fig. 4 b)) was not affected and the total water vapor net
157 flux was negligible for the analyzed volume. Continued sublimation and deposition of
158 water molecules due the Kelvin-effect led to a saturation of the pore space. The vapor
159 pressure of the air in the pore was in equilibrium with the water pressure of the ice, given
160 by the local temperature. However, the uptake of water molecules and their transport due
161 to warming during propagation was counteracted by diffusion of water molecules due to

162 the temperature gradient. As thermally induced diffusion was opposite to the airflow gra-
 163 dient, a backflow of water vapor occurred and the two opposite fluxes cancelled each
 164 other out. The Peclet numbers ($Pe = u_D \cdot d_{\text{mean}} / D$ where D is the diffusion coefficient of
 165 water vapor in air), describing the ratio of mass transfer between diffusion and advection,
 166 measured during each experiment, showed that diffusion was still dominant (Table 1).
 167 Therefore, water molecules were diffused along the temperature gradient and advected
 168 along the flow direction leading to a back and forth transport of water molecules.

169 As a Peclet higher than 1 is not possible in nature (Ebner et al., 2015a), advection of
 170 cold saturated air into a slightly warmer snowpack has a significant influence not on the
 171 total net mass change but on the structural change of the ice grains due to redistribution
 172 of water vapor on the ice matrix. Also the increasing pore size has an influence on the
 173 flow field leading to a deceleration of the flow and therefore the interaction of an air-
 174 parcel with the ice matrix in the pores increases due to higher residence time. In addition,
 175 the diffusive transport rises whereas the advective transport decreases changing the mass
 176 transport in the pores. Our results support the hypothesis of Neumann et al. (2009) that
 177 sublimation is limited by vapor diffusion into the pore space rather than sublimation at
 178 crystals faces. This is also supported by the temporal evolution of the porosity (Fig. 4 b))
 179 and the SSA (Fig. 4 c)), as no velocity dependence was observed and the structural
 180 changes were too small to be detected by the micro-CT.

181 The influence of diffusion of water vapor in the direction of the temperature gradient
 182 and the influence of the residence time of an air-parcel in the pores were also confirmed
 183 by a low mass change at the ice-air interface. Overlapping two consecutive 3D images,
 184 the order of magnitude of freshly sublimated ice was detected. The absolute mass change
 185 at the ice-air interface ($\text{kg m}^{-3} \text{s}^{-1}$) estimated by the experimental results is defined as

$$186 \quad S_{\text{m,exp}} = \left| \rho_i \frac{\Delta(1-\varepsilon)}{\Delta t} \right| \quad (1)$$

187 where $\Delta(1-\varepsilon)$ is the change in the porosity between two images separated by the time step
 188 Δt , and ρ_i is the density of ice. Albert and McGilvary (1992) and Neumann et al. (2009)
 189 presented a model to calculate sublimation rates directly in an aggregate snow sample

$$190 \quad S_{\text{m}} = |h_{\text{m}} \text{SA}_{\text{v}} (\rho_{\text{sat}} - \rho_{\text{v}})| \quad (2)$$

191 where SA_{v} is the specific surface area per volume of snow, and h_{m} is the mass-transfer
 192 coefficient (m s^{-1}) given by (Neumann et al., 2009)

$$193 \quad h_{\text{m}} = (0.566 \cdot \text{Re} + 0.075) \cdot 10^{-3} \quad (3)$$

194 assuming that the sublimation occurs within the first few mm of the sample. Re ($Re =$
195 $u_D \cdot d_{\text{mean}} / \nu$ where ν is the kinematic viscosity of the air) is the corresponding Reynolds-
196 number of the flow. The absolute sublimation rate is driven by the difference between the
197 local vapor density (ρ_v) and the saturation vapor density (ρ_{sat}) (Neumann et al., 2009;
198 Thorpe and Mason, 1966). Table 2 shows the estimated absolute sublimation rate by the
199 experiment (Eq. (1)) and the model (Eq. (2)). The very small change in porosity due to
200 densification during the first 18 h for ‘ota2’ was not taken into account. The estimated
201 sublimation rates by the experiment were two orders of magnitude lower than the mod-
202 elled values and also two orders of magnitude lower than for the temperature gradient
203 along an airflow experiment (Ebner et al., 2015b). As the air in the pore spaces is always
204 saturated (Neumann et al., 2009), the back diffusion of water vapor in the direction of the
205 temperature gradient led to a lower mass transfer rate of sublimation. The flow rate de-
206 pendence for the model described is shown by the mass-transfer coefficient (Eq. 3), in-
207 creasing with higher airflow. However, the values calculated from the experiment showed
208 a different trend. Increasing the flow rate led to a lower mass transfer rate due to a lower
209 residence time of the air in the pores. Transfer of heat toward and water vapor away from
210 the sublimating interface may also limit the sublimation rate. In general, the results of the
211 model by Neumann et al. (2009) have to be interpreted with care, as the model was set up
212 to saturate dry air under isothermal conditions. Ice crystals sublimated as dry air enters
213 the snow sample; water vapor was advected throughout the pore space by airflow until
214 saturation vapor pressure was reached, preventing further sublimation. The model by
215 Neumann et al. (2009) does not consider the influence of a temperature gradient and the
216 additional vapor pressure gradient was not analyzed.

217 In the experiments by Neumann et al. (2009), sublimation of snow using dry air under
218 isothermal condition showed a temperature drop for approximately the first 15 min after
219 sublimation began and stayed constant because the latent heat absorption of sublimation
220 for a given flow rate and heat exchange with the sample chamber equalized each other.
221 Such a temperature drop was not observed in our experiments. In the experiments by
222 Neumann et al. (2009) the amount of energy used for sublimation was between -10 and -
223 40 J min^{-1} for saturation of dry air. Using the expected mass change at the ice-air interface
224 $S_{\text{m,exp}}$ (Eq. (1)) and the latent heat of sublimation ($L_{\text{sub}} \approx 2834.1 \cdot 10^3 \text{ J kg}^{-1}$) the energy
225 needed for sublimation ranged between -2 and -12 J min^{-1} for our experiments. Our esti-
226 mated values are a factor up to five lower than the estimated numbers of Neumann et al.

227 (2009), because the entering air was already saturated (with reference to the cold temper-
228 ature) at the inlet. The needed energy for sublimation could be balanced between the sen-
229 sible heat carried into and out of the sample, and the exchange of the snow sample with
230 the air stream and the surrounding prevented a temperature drop.

231 Thermal conductivity changed insignificantly in these experiments. This indicates
232 that advective cold airflow opposite to a temperature gradient and an open system reduces
233 or suppresses the increase in thermal conductivity usually observed by temperature gra-
234 dient metamorphism (Riche and Schneebeli, 2013).

235

236 **6. Summary and conclusion**

237 We performed four experiments of temperature-gradient metamorphism of snow un-
238 der saturated advective airflow during 108 h. Cold saturated air was blown into the snow
239 samples and warmed up while flowing across the sample. The temperature gradient varied
240 between 43 and 53 K m⁻¹ and the snow microstructure was observed by X-ray micro-
241 tomography every 3 h. The micro-CT scans were segmented, and porosity, specific sur-
242 face area, and the mean pore-size were calculated. Effective thermal conductivity was
243 calculated in direct pore-level simulations (DPLS).

244 Compared to deposition (shown in Ebner et al., 2015b), sublimation showed a small
245 effect on the structural change of the ice matrix. A change in the pore size was most likely
246 due to sublimation of ice crystal with low radii but a significant loss of water molecules
247 of the snow sample and mass transfer away from the ice interface due to sublimation and
248 advective transport could not be detected by the micro-CT scans and no flow rate depend-
249 ence was observed. The interaction of mass transport of advection and diffusion of water
250 vapor in the direction of the temperature gradient and the influence of the residence time
251 of an air-parcel in the pores led to a negligible total mass change of the ice. However, a
252 strong reposition of water molecules on the ice grains was observed.

253 The kinetic phase-change from gas to solid is preferable as energy is released com-
254 pared to solid to gas where energy is required, thus leading to more water molecule dep-
255 osition than water molecule sublimation. The energy needed for sublimation was too low
256 to see a significant temperature drop because the needed energy was balanced between
257 the sensible heat carried into and out of the sample, and the exchange of the snow sample
258 with the air stream and the surrounding.

259 This is the third paper of a series analyzing an advective airflow in a snowpack. Pre-
260 vious work showed that: (1) under isothermal conditions Kelvin-effect leads to a satur-
261 ation of the pore space in the snow but did not affect the structural change. (Ebner et al.,
262 2015a); (2) applying a temperature gradient along the flow direction leads to a change in
263 the microstructure and creation of whistler-like structures due to deposition of water mol-
264 ecules on the ice matrix (Ebner et al., 2015b); and (3) a temperature gradient opposed to
265 the flow had a negligible total mass change of the ice but a strong reposition effect of
266 water molecules on the ice grains, shown in this paper. Conditions (1) and (3) showed
267 that they have a negligible effect on the porosity evolution of the ice matrix and can be
268 neglected to improve models for snow compaction and evolution at the surface. In con-
269 trast, conditions (2) showed a significant impact on the structural evolution and seems to
270 be essential for such snowpack models and other numerical simulations. Nevertheless,
271 the strong reposition of water molecules on the ice grains observed for all conditions (1)
272 – (3) can have a significant impact on atmospheric chemistry and isotope contents in
273 snow.

274

275 **Acknowledgements**

276 The Swiss National Science Foundation granted financial support under project Nr.
277 200020-146540. The authors thank the reviewers E. A. Podolskiy and F. Flin for the sug-
278 gestions and critical review and M. Jaggi, S. Grimm, H. Löwe for technical and modelling
279 support.

280

281 **References**

- 282 Albert, M. R.: Effects of snow and firn ventilation on sublimation rates, *Annals of Glac-*
283 *iology*, 35, 52-56, 2002.
- 284 Albert, M. R. and Hardy, J. P.: Ventilation experiments in a seasonal snow cover, in *Bi-*
285 *ogeochemistry of Seasonally Snow-Covered Catchments*, IAHS Publ. 228, edited by
286 K. A. Tonnessen, M. W. Williams, and M. Tranter, 41 –49, IAHS Press, Wallingford,
287 UK, 1995.
- 288 Albert, M. R. and McGilvary, W. R.: Thermal effects due to air flow and vapor transport
289 in dry snow, *Journal of Glaciology*, 38, 273-281, 1992.

290 Box, J. E. and Steffen, K.: Sublimation on the Greenland ice sheet from automated
291 weather station observations, *Journal of Geophysical Research*, 107, 33965-33981,
292 2001.

293 Calonne, N, Flin, F., Morin, S., Lesaffre, B., and Rolland du Roscoat, S.: Numerical and
294 experimental investigations of the effective thermal conductivity of snow, *Geophys-*
295 *ical Research Letter*, 38, 1-6, 2011.

296 Calonne, N., Geindreau, C., Flin, F., Morin, S., Lesaffre, B., Rolland du Roscoat, S., and
297 Charrier, P.: 3-D image-based numerical computations of snow permeability: links
298 to specific surface area, density, and microstructural anisotropy, *The Cryosphere*, 6,
299 939-951, 2012.

300 Chen, S., and Baker, I.: Evolution of individual snowflakes during metamorphism, *Jour-*
301 *nal of Geophysical Research*, 115, 1–9, 2010.

302 Colbeck, S. C.: Air movement in snow due to windpumping, *Journal of Glaciology*, 35,
303 209–213, 1989.

304 Déry, S. J. and Yau, M. K.: Large-scale mass balance effects of blowing snow and surface
305 sublimation, *Journal of Geophysical Research*, 107, doi:10.1029/2001JD001251,
306 2002.

307 Ebner, P. P., Grimm, S., Schneebeli, M., and Steinfeld, A.: An instrumented sample
308 holder for time-lapse micro-tomography measurements of snow under advective con-
309 ditions, *Geoscientific Instrumentation Methods and Data Systems*, 3, 179–185, 2014.

310 Ebner, P. P, Schneebeli, M., and Steinfeld, A.: Tomography-based observation of isother-
311 mal snow metamorphism under advective conditions, *The Cryosphere*, 9, 1363–
312 1371, 2015a.

313 Ebner, P. P, Andreoli, C., Schneebeli, M., and Steinfeld, A.: Tomography-based obser-
314 vation of ice-air interface dynamics of temperature gradient snow metamorphism un-
315 der advective conditions, *Journal of Geophysical Research*, submitted, 2015b.

316 Ekaykin, A. A., Hondoh, T., Lipenkov, V. Y., and A. Miyamoto: Post-depositional
317 changes in snow isotope content: preliminary results of laboratory experiments,
318 *Clim. Past Discuss.*, 5, 2239–2267, 2009.

319 Gjessing, Y. T.: The filtering effect of snow, in: *Isotopes and Impurities in Snow and Ice*
320 *Symposium*, edited by: Oeschger, H., Ambach, W., Junge, C. E., Lorius, C., and
321 Serebryanny, L., 118, IASH-AISH Publication, Dorking, 199–203, 1977.

322 Haussener, S., Gergely, M., Schneebeli, M., and Steinfeld, A.: Determination of the mac-
323 roscopic optical properties of snow based on exact morphology and direct pore-level
324 heat transfer modeling, *Journal of Geophysical Research*, 117, 1–20, 2012.

325 Kaempfer, T. U., Schneebeli, M. and Sokratov, S. A.: A microstructural approach to
326 model heat transfer in snow, *Geophysical Research Letter*, 32, 1–5, 2005.

327 Kaempfer, T. U. and Plapp, M.: Phase-field modeling of dry snow metamorphism, *Phys-*
328 *ical Review E*, 79, <http://dx.doi.org/10.1103/PhysRevE.79.031502>, 2009.

329 Löwe, H., Spiegel, J. K., and Schneebeli, M.: Interfacial and structural relaxations of
330 snow under isothermal conditions, *Journal of Glaciology*, 57, 499–510, 2011.

331 Löwe, H., Riche, F., and Schneebeli, M.: A general treatment of snow microstructure
332 exemplified by an improved relation for the thermal conductivity, *The Cryosphere*
333 *Discussions*, 6, 4673–4693, (2012).

334 Neumann, T. A., Albert, M. R., Lomonaco, R., Engel, C., Courville, Z., and Perron, F.:
335 Experimental determination of snow sublimation rate and stable-isotopic exchange,
336 *Annals of Glaciology*, 49, 1–6, 2008

337 Neumann, T. A., Albert, M. R., Engel, C., Courville, Z., and Perron, F.: Sublimation rate
338 and the mass-transfer coefficient for snow sublimation, 52, 309–315, 2009.

339 Otsu, N.: A Threshold Selection Method from Gray-Level Histograms, *IEEE Transac-*
340 *tions on Systems Man and Cybernetics*, 9, 62–66, 1979.

341 Petrasch, J., Schrader, B., Wyss, P., and Steinfeld, A.: Tomography-based determination
342 of effective thermal conductivity of fluid-saturated reticulate porous ceramics, *Jour-*
343 *nal of Heat Transfer*, 130, 1–10, 2008.

344 Pinzer, B. R., and Schneebeli, M.: Snow metamorphism under alternating temperature
345 gradients: Morphology and recrystallization in surface snow, *Geophysical Research*
346 *Letters*, 36, 1–4, 2009.

347 Pinzer, B. R., Schneebeli, M., and Kaempfer, T. U.: Vapor flux and recrystallization dur-
348 ing dry snow metamorphism under a steady temperature gradient as observed by
349 time-lapse micro-tomography, *The Cryosphere*, 6, 1141–1155, 2012.

350 Riche, F. and Schneebeli, M.: Thermal conductivity of snow measured by three independ-
351 ent methods and anisotropy considerations, *The Cryosphere*, 7, 217–227, (2013).

352 Schleef, S., Jaggi, M., Löwe, H., and Schneebeli, M.: Instruments and Methods: An im-
353 proved machine to produce nature-identical snow in the laboratory, *Journal of Glac-*
354 *iology*, 60, 94–102, 2014.

355 Stichler, W., Schotterer, U., Frohlich, K., Ginot, P., Kull, C., Gäggeler, H., and Pouyaud,
356 P.: Influence of sublimation on stable isotope records recovered from high-altitude
357 glaciers in the tropical Andes, *Journal of Geophysical Research*, 106, 22613-22630,
358 2001.

359 Sturm, M. and Benson, C.: Vapor transport grain and depth-hoar development in the sub-
360 arctic snow, *Journal of Glaciology*, 43, 42-59, 1997.

361 Sturm, M., and Johnson, J. B.: Natural convection in the subarctic snow cover, *Journal of*
362 *Geophysical Research*, 96, 11657–11671, 1991.

363 Thorpe, A. D. and Mason, B. J.: The evaporation of ice spheres and ice crystals, *British*
364 *Journal of Applied Physics*, 17, 541-548, 1966.

365 Waddington, E. D., Cunningham, J., and Harder, S. L.: The effects of snow ventilation
366 on chemical concentrations, in: *Chemical Exchange Between the Atmosphere and*
367 *Polar Snow*, edited by: Wolff, E. W. and Bales, R. C., NATO ASI Series, 43,
368 Springer, Berlin, 403–452, 1996.

369 Wang, X. and Baker, I.: Evolution of the specific surface area of snow during high-tem-
370 perature gradient metamorphism, *Journal of Geophysical Research Atmosphere.*,
371 119, 13690–13703, 2014

372

373 **Table 1:** Morphological and flow characteristics of the experiments: Volume flow (\dot{V}),
374 initial superficial velocity in snow ($u_{D,0}$), initial snow density (ρ_0), initial porosity (ε_0),
375 specific surface area (SSA_0), initial mean pore size (d_{mean}), average inlet ($T_{\text{in,ave}}$) and outlet
376 temperature ($T_{\text{out,ave}}$), and the average temperature gradient (∇T_{ave}), corresponding Reyn-
377 olds number (Re) and Peclet number (Pe).

378

Name	\dot{V} liter min ⁻¹	$u_{D,0}$ m s ⁻¹	ρ_0 kg m ⁻³	ε_0 –	SSA_0 m ² kg ⁻¹	d_{mean} mm	$T_{\text{in,ave}}$ °C	$T_{\text{out,ave}}$ °C	∇T_{ave} K m ⁻¹	Re –	Pe –
ota1	–	–	284.3	0.69	25.0	0.30	-13.8	-12.5	43.3	–	–
ota2	0.3	0.004	256.8	0.72	26.3	0.33	-14.0	-12.5	50.0	0.07	0.05
ota3	1.0	0.012	256.8	0.72	24.3	0.34	-13.8	-12.3	43.3	0.25	0.19
ota4	3.0	0.036	265.9	0.71	21.7	0.36	-14.6	-13.0	53.3	0.78	0.61

379

380

381

382 **Table 2:** Estimated sublimation rate S_m using the mass transfer coefficient h_m determined
383 by Neumann et al. (2009) and the corresponding average surface area per volume $SA_{V,\text{ave}}$.
384 S_m can be compared with the measured sublimation rate of the experiment $S_{m,\text{exp}}$ (Eq. (1)).

385

Name	$SA_{V,\text{ave}}$ mm ⁻¹	h_m m s ⁻¹	S_m kg m ⁻³ s ⁻¹	$S_{m,\text{exp}}$ kg m ⁻³ s ⁻¹
ota1	22.44	$0.75 \cdot 10^{-4}$	$4.83 \cdot 10^{-4}$	$0.68 \cdot 10^{-6}$
ota2	23.98	$1.15 \cdot 10^{-4}$	$2.99 \cdot 10^{-4}$	$4.48 \cdot 10^{-6}$
ota3	21.88	$2.17 \cdot 10^{-4}$	$5.15 \cdot 10^{-4}$	$0.76 \cdot 10^{-6}$
ota4	19.61	$5.16 \cdot 10^{-4}$	$10.9 \cdot 10^{-4}$	$0.08 \cdot 10^{-6}$

386

387 **Figure captions**

388 **Fig. 1.** Schematic of the ice-air interface transport processes: a) Under isothermal
389 conditions Kelvin-effect leads to a saturation of the pore space in the snow
390 but did not affect the structural change (Ebner et al., 2015a); b) Temperature
391 gradient along the flow direction leads to a change in the microstructure due
392 to deposition (Ebner et al., 2015b); c) Temperature gradient opposite to the
393 flow has a negligible total mass change of the ice but a strong reposition effect
394 of water molecules on the ice grains, shown in this paper.

395 **Fig. 2.** Evolution of the 3-D structure of the ice matrix with applied temperature gra-
396 dient and advective conditions. Experimental conditions (from left to right) at
397 different measurement times from beginning to the end (top to bottom) of the
398 experiment. The shown cubes are $110 \times 40 \times 110$ voxels ($2 \times 0.7 \times 2 \text{ mm}^3$)
399 large with $18 \mu\text{m}$ voxel size (a high resolution figure can be found in supple-
400 mentary material).

401 **Fig. 3.** Superposition of vertical cross-section parallel to the flow direction at time 0
402 and 108 hours for ‘ota3’ (left panel) and ‘ota4’ (right panel). Sublimation and
403 deposition of water vapor on the ice grain were visible with an uncertainty of
404 6 % (a high resolution figure can be found in supplementary material).

405 **Fig. 4.** Temporal evolution of a) the mean pore size, d_{mean} , of the snow samples ob-
406 tained by opening-size distribution, b) the porosity, ε , obtained by triangu-
407 lated structure surface method, c) the specific surface area, SSA, of the ice
408 matrix obtained by triangulated structure surface method, and d) the effective
409 thermal conductivity of the snow sample, k_{cond} , estimated by DPLS simula-
410 tions.

411

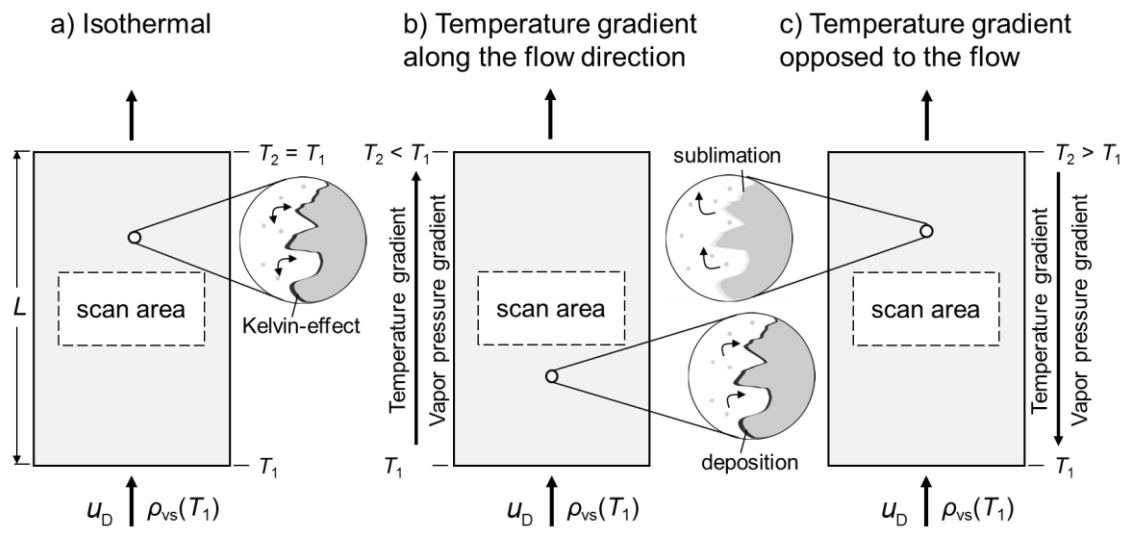


Fig. 1

412

413

414

415

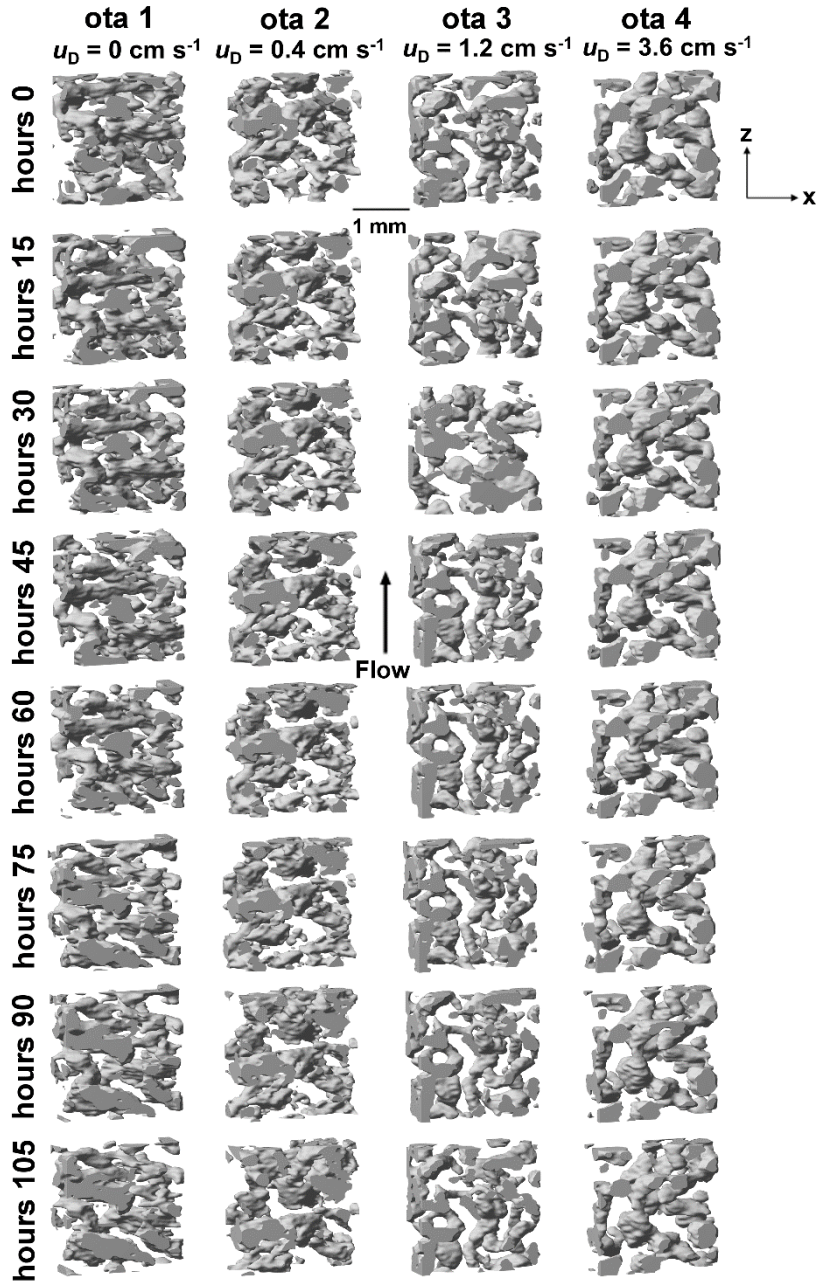


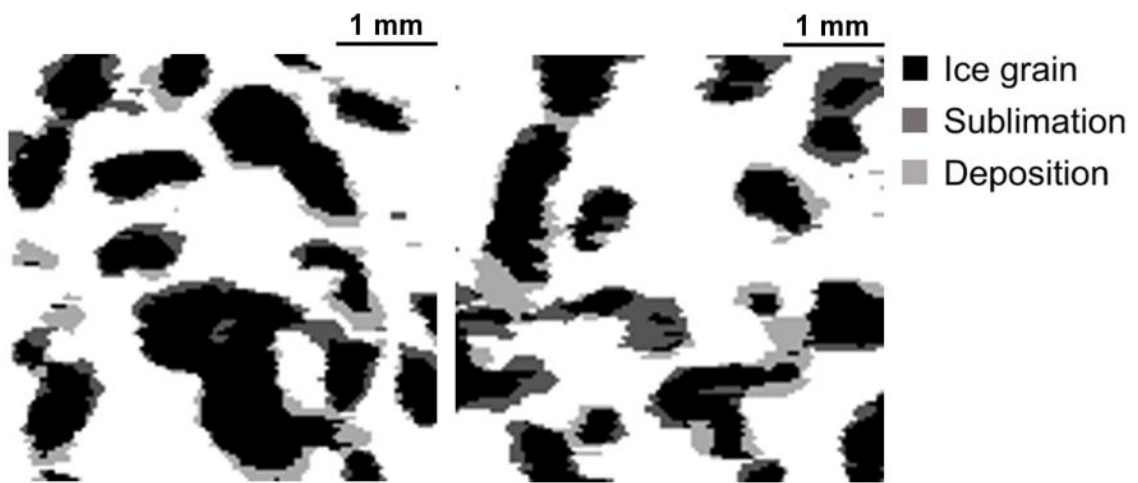
Fig. 2

416

417

418

419



420

421

422

Fig. 3

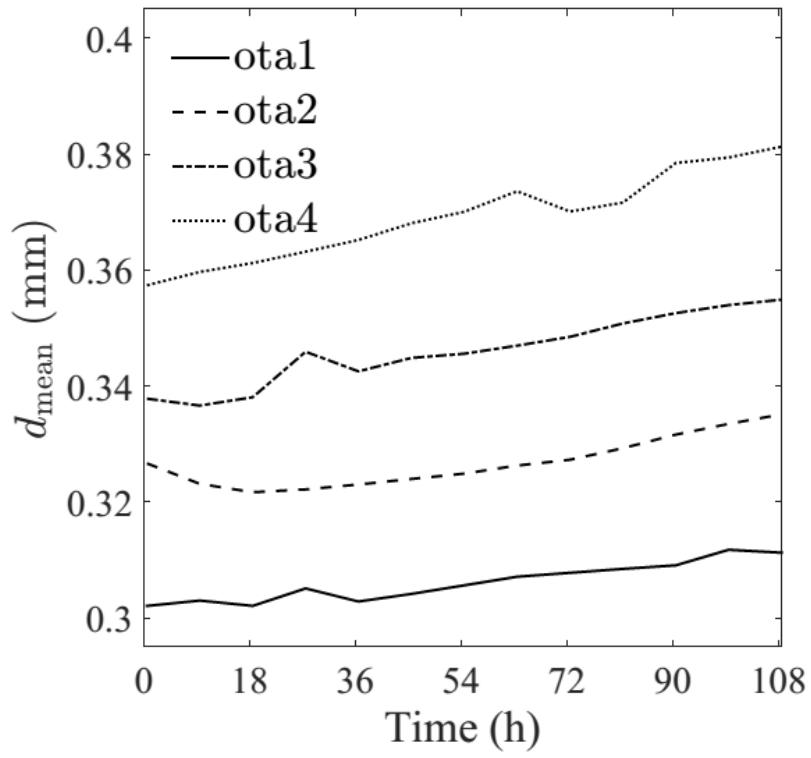


Fig. 4 a)

423

424

425

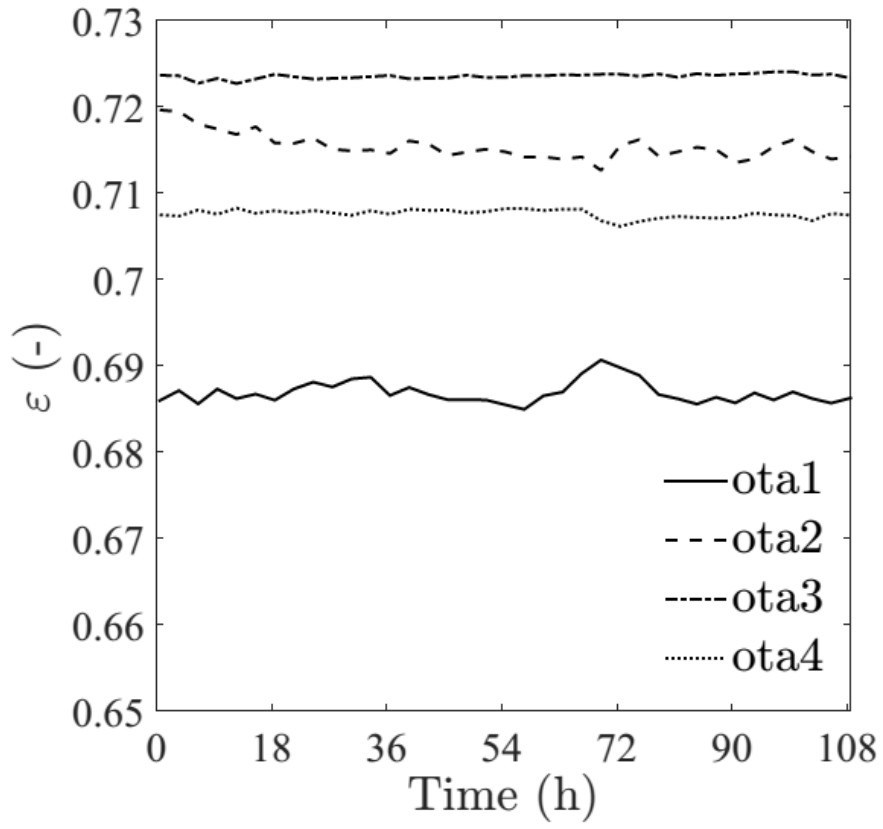


Fig. 4 b)

426

427

428

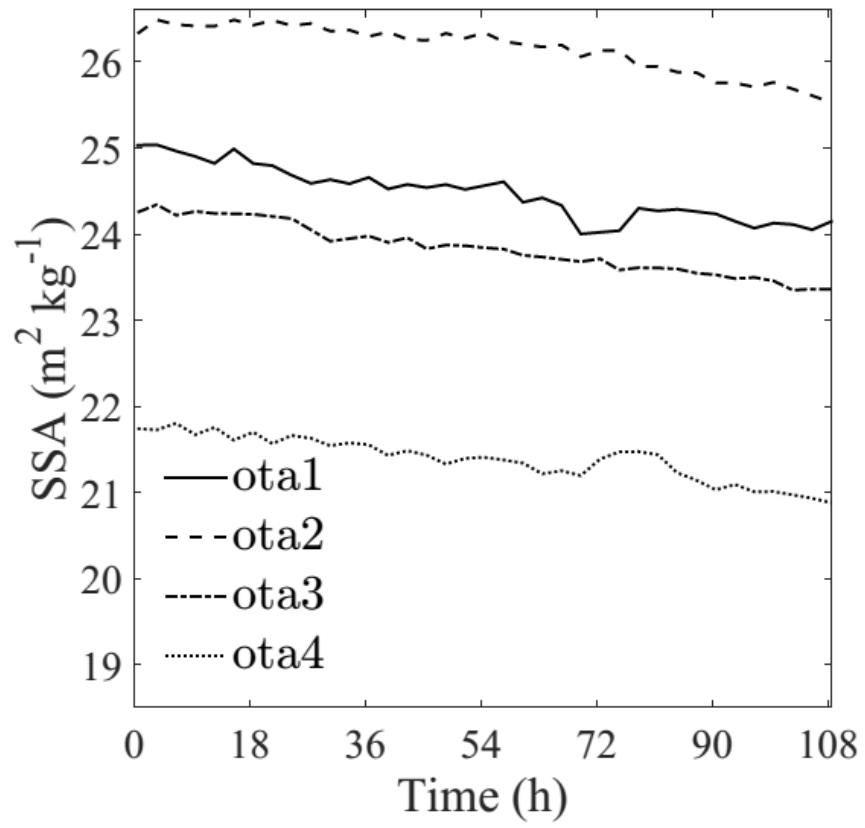
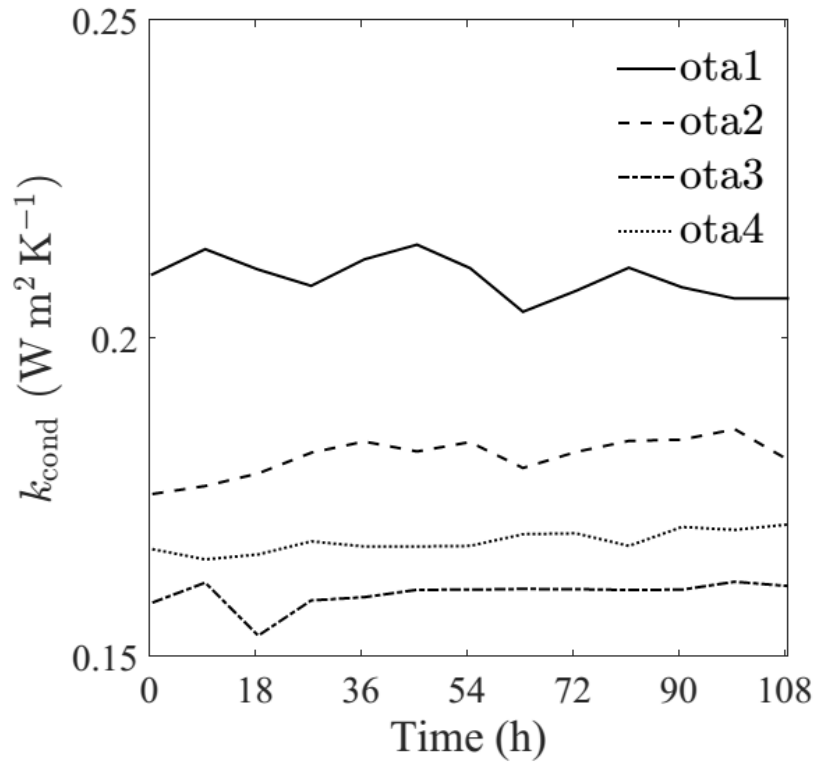


Fig. 4 c)

429

430

431



432

433

Fig. 4 d)